

Score-based Integrated Gradient for Root Cause Explanations of Outliers

Phuoc Nguyen, Truyen Tran, Sunil Gupta, Svetha Venkatesh

Applied Artificial Intelligence Initiative (A2I2)

Deakin University, Australia

{phuoc.nguyen,truyen.tran,sunil.gupta,svetha.venkatesh}@deakin.edu.au

Abstract—Identifying the root causes of outliers is a fundamental problem in causal inference and anomaly detection. Traditional approaches based on heuristics or counterfactual reasoning often struggle under uncertainty and high-dimensional dependencies. We introduce SIREN, a novel and scalable method that attributes the root causes of outliers by estimating the score functions of the data likelihood. Attribution is computed via integrated gradients that accumulate score contributions along paths from the outlier toward the normal data distribution. Our method satisfies three of the four classic Shapley value axioms—dummy, efficiency, and linearity—as well as an asymmetry axiom derived from the underlying causal structure. Unlike prior work, SIREN operates directly on the score function, enabling tractable and uncertainty-aware root cause attribution in nonlinear, high-dimensional, and heteroscedastic causal models. Extensive experiments on synthetic random graphs and real-world cloud service and supply chain datasets show that SIREN outperforms state-of-the-art baselines in both attribution accuracy and computational efficiency.

Index Terms—Score matching, integrated gradient, root causes, anomaly detection.

I. INTRODUCTION

Identifying the root causes of outliers in complex network systems is critical across diverse domains, including manufacturing, cloud services, and distributed computing. Effective root cause analysis facilitates timely interventions, restores normal operations, and prevents costly failures. For example, in modern manufacturing, even brief system downtime can incur substantial economic losses [1]. However, pinpointing the root causes of anomalies is particularly challenging in high-dimensional and noisy monitoring data, which is often exacerbated by random fluctuations and system delays [2–5].

Recent causal inference approaches leverage underlying dependency structures among variables to systematically attribute anomalies to their upstream causes [6–10]. Central to these approaches is a principled measure of “outlierness,” which can be effectively decomposed according to the causal graph. For instance, [8] frames outlier attribution within an information-theoretic context, employing Shapley values to quantify contributions by averaging marginal effects across variable subsets. Similarly, [11] utilizes the norm of the score function (gradient of the log density) as an information-based measure of anomaly severity.

Despite their successes, existing methods face significant practical limitations. Shapley-based approaches are computationally intensive due to combinatorial subset evaluations and

may produce inconsistent, off-manifold samples. Additionally, these methods require access to original training data as empirical distributions for attribution methods such as Shapley values, raising concerns regarding data storage and privacy [12, 13]. Integrated gradient methods, such as those proposed by [9], offer computational advantages but are limited to linear Gaussian models.

To overcome these limitations, we propose **SIREN** (short hand for Score-based Integrated Gradient Root Cause Explanation), a novel framework that integrates conditional score modeling with diffusion-based integrated gradients. SIREN estimates the score function of data distributions conditioned on a causal structure with additive noise. We decompose the score function into a deterministic mean component and a noise-conditioned component. This allows for efficient and principled attribution of anomalies without reliance on training data at inference time. SIREN extends existing approaches by accommodating both linear and nonlinear functional causal models with heteroscedastic noise sources. Our framework reinterprets outliers as violations of causal invariance rather than merely extreme noise realizations, offering deeper insights into context-sensitive changes in system mechanisms.

Our framework relies on standard causal assumptions: data generated by a Functional Causal Model (FCM) structured as a directed acyclic graph (DAG) under causal sufficiency and independent exogenous noise terms. We assume the noise score functions are locally estimable, enabling efficient gradient-based inference along reverse-time diffusion trajectories.

Our primary contributions include:

- 1) A conditional score estimation approach leveraging causal structures to sample gradient-based attribution paths efficiently and without access to training data.
- 2) A computationally efficient decomposition of the score function into mean and noise-conditioned components, facilitating scalable attribution.
- 3) Establishing a theoretical link between our integrated gradient method and Shapley value theory, explicitly relating attribution scores to differences in tail probabilities.
- 4) Applicability to nonlinear additive noise models with arbitrary differentiable noise distributions, significantly broadening the range of practical use cases.

II. PRELIMINARIES

We summarize the background and notations needed for our study in this section. We use capital letters for random variables and lowercase letters for observations.

A. Outlier Measures

Outlier measures are crucial in identifying the root causes of outliers. From the information theory point of view, [8] defines an outlier measure of observing an event $X = x$ as:

$$S_X(x) = -\log P\{-\log p_X(X) \geq -\log p_X(x)\}, \quad (1)$$

where X has density $p_X(X)$, and $P(Y)$ is the distribution of the “information” $Y = -\log p_X(X)$. By using the information space of Y instead of the input space of X , this scoring function can characterize outliers in multivariate data and multimodal distributions. In addition, it has the property that high measures corresponding to low-density regions between clusters of data, which only contain rare events significantly less represented compared to the majority of data points [8].

B. Functional Causal Models (FCMs)

We assume there exists a true data generating process governed by a causal structure represented by a directed acyclic graph G . The nodes of the graph represent the variables generating the real world observations, and the directed edges from the parent nodes to a node indicate the causal dependence of that node on its parents. This causal relationship can be captured in the following functional causal mechanism [14, 15]:

The causal mechanism for each variable is represented using a functional causal model (FCM), which takes the general form:

$$X_j = f_j(\mathbf{Pa}_j, Z_j), \quad (2)$$

where f_j is a deterministic function capturing the systematic influence of the parents on X_j , and $Z_j \sim P(Z_j)$ is an independent noise variable specific to node j .

1) *Additive Noise Model (ANM)* [16, 17]: In this model, the noise source Z_j enters Eq. 2 additively:

$$X_j = f_j(\mathbf{Pa}_j) + Z_j, \quad (3)$$

where the noise Z_j is a general homoscedastic, zero-mean, and independent of the inputs. Together, the mean function f_j and the noise Z_j define the causal mechanism for node j . In practice, the functional form of the $\{f_j\}$ can be determined using domain knowledge or selected from an approximation family, such as linear regression models [8, 18] or Bayesian linear regression models [9]. These models can then be fitted to observational data $D = \{\mathbf{x}^{(i)}\}_{i=1}^m$. The noise is assumed to follow a zero-mean distribution—commonly Gaussian, but potentially uniform or any other zero-mean form. Model parameters can be learned by fitting the residuals $X_j^{(i)} - f_j(\mathbf{Pa}_j^{(i)})$, assuming

$$X_j^{(i)} \sim \mathcal{N}(f_j(\mathbf{Pa}_j^{(i)}), \sigma_j^2),$$

where σ_j^2 is constant.

2) *Location-scale Noise Model (LSN)* [19]: In practice, noise may not enter purely additively or with fixed variance. A more general and realistic class of models is the location-scale noise model [19], in which both the mean and variance of the noise can vary with the parents:

$$X_j = f_j(\mathbf{Pa}_j) + \sigma_j(\mathbf{Pa}_j) \cdot Z_j \quad (4)$$

This formulation generalizes ANMs by incorporating heteroscedasticity—i.e., noise variance that depends on the input. This flexibility enables the model to capture real-world phenomena such as supply chain delay and financial volatility. These models can be fitted to observational data $D = \{\mathbf{x}^{(i)}\}_{i=1}^m$ by maximizing the likelihood of the Gaussian model

$$X_j^{(i)} \sim \mathcal{N}(f_j(\mathbf{Pa}_j^{(i)}), \sigma_j^2(\mathbf{Pa}_j^{(i)})),$$

where f_j and σ_j^2 are parameterized functions learned from data. Together, the mean function f_j , the scale function σ_j , and the noise Z_j define the causal mechanism for node j with heteroscedasticity noises.

C. Root Cause Attributions

Based on a given causal structure, [8] proposed a method to identify root causes by attributing the outlier measure observed at a target leaf node to the independent noise source of every node. The authors first fit the FCMs to the normal observational data, then inverse the independent noises z_j from this observational data by computing the residuals

$$z_j = x_j - f_j(\mathbf{x}_{\mathbf{Pa}_j}) \quad (5)$$

In order to use the Shapley attribution method [20, 21] to explain an outlier event at a leaf $x_n = f_n(\mathbf{Pa}_n, z_n)$, the authors expand the FCMs to express x_n as a function depending directly on all these noise variables¹:

$$x_n = f(z_1, \dots, z_n) = f(\mathbf{z}) \quad (6)$$

In this way, the noise variables \mathbf{z} play the role of selecting deterministic mechanisms.

We clarify the sentence by grounding it in the canonical representation of Functional Causal Models (FCMs), as in Peters et al. (2017, Ch. 3). In this view, the structural equation

$$Y := f(X, Z)$$

can equivalently be seen as a stochastic function over X , where the exogenous noise Z selects a deterministic function. More precisely, if we fix $Z = z$, then Y becomes a deterministic function

$$Y := f_z(X) = f(X, z),$$

so the noise Z selects which deterministic response function governs the relationship between X and Y . Thus, Z induces a distribution $P(Z)$ over the function space Y^X , turning the FCM into $Y := Z(X)$, where $Z \in Y^X$ is a random function. In this response function representation, the noise no longer

¹where we abuse notation and denote the same f to mean the same data generating process but rewritten to take input \mathbf{z}

perturbs the output directly, but selects which mechanism (function) maps inputs to outputs.

In this formulation, each draw of the noise variable z corresponds to selecting a deterministic mechanism f_z , turning the stochastic FCM into a distribution over deterministic functions from inputs to outputs.

Thus, an outlier mechanism j will be determined by an outlier noise z_j and is likely to be the root cause of an observed outlier x_n at leaf n . Note that the outlier measure in Eq. 1 for the leaf n will depend on the noise \mathbf{z} as follows:

$$\begin{aligned} S_{X_n}(x_n) &= -\log P\{-\log p(X_n) \geq -\log p(x_n)\} \\ &= -\log P\{-\log p(f(\mathbf{Z})) \geq -\log p(f(\mathbf{z}))\} \end{aligned} \quad (7)$$

where the residual \mathbf{z} is calculated using Eq. 5. To determine the real contribution of each node j to the leaf node outlier measure $S_{X_n}(x_n)$, its sensitivity w.r.t. to an ancestor node j need to be taken into account given the context of the remaining noise sources $\mathbf{z}_{N \setminus j}$. For this purpose, the authors use Shapley values [20, 21] a concept from cooperative game theory to correctly measure the contribution of each noise term to $S_{X_n}(x_n)$.

a) *Shapley Values*: Here, the n noises $\mathbf{z} = \{z_1, \dots, z_n\}$ are assumed to play a game by propagating their values through the FCMs and eventually contributing to the outlier measure $S_{X_n}(x_n)$. Let $v : 2^n \rightarrow \mathbb{R}$ be a value function [22] which map a subset $I \subseteq N$ of noise variables to a real number representing the final outlier measure caused by this coalition I . The value function is defined as [23]:

$$v(I) = \mathbb{E}_{p_Z(z')} [S_{X_n}(z_I \cup z'_I)] \quad (8)$$

where $\bar{I} = N \setminus I$ is the out-of-coalition set whose noises, z'_I , are marginalized out, and the outlier measure $S_{X_n}(\mathbf{z})$ at leaf n is defined as in Eq. 7. The target value $v(N)$ where all observed noises are considered can then be uniquely decomposed as

$$v(N) = v(\{\}) + \sum_{j \in N} \phi_v(j) \quad (9)$$

where $v(\{\})$ is the baseline value of empty set when no noise is considered, i.e. marginalized out, and $\phi_v(j)$ is the Shapley value of each node j . This Shapley value is defined as [21]:

$$\phi_v(j) = \sum_{I \subseteq N \setminus j} \frac{|I|!(n - |I| - 1)}{n!} \phi_v(j|I), \quad (10)$$

$$\text{and } \phi_v(j|I) = v(I \cup j) - v(I) \quad (11)$$

where $\phi_v(j)$ is the marginal Shapley value by averaging over all possible coalitions, and $\phi_v(j|I)$ is the Shapley value of node j given the coalition I . In practice, it is typical to use subset sampling of the orderings to reduce computation. Eq. 10 shows that the Shapley value $\phi_v(j)$ represents the marginal contribution of the node j .

b) *Integrated Gradient (IG)*: Instead of using Shapley values, [9] proposed to use integrated gradient (IG) [23] to compute the outlier measure attributions to each noise variable z_j . This method requires a noise reference which can be sampled from the normal noise distribution $\mathbf{z}' \sim p_Z$ to explain the root cause of an outlier observation $x_n = f(\mathbf{z})$. The attribution value of node i is defined as line integral:

$$\text{IG}_j(\mathbf{z}, \mathbf{z}') = (z_j - z'_j) \int_{t=0}^1 \frac{\partial S_{X_n}(\mathbf{z}(t))}{\partial z_j} dt \quad (12)$$

where the line $\mathbf{z}(t) = \mathbf{z}' + t(\mathbf{z} - \mathbf{z}')$, and S_{X_n} is the outlier measure function in Eq. 1. This attribution function computes the contribution of the noise z_i to the final outlier measure by integrating the gradient of the outlier measure along the line from z_i to the reference z'_i , hence the name IG. In practice, the continuous path is discretized for Riemann integration.

III. METHODS

A. Score-based Integrated Gradient

Instead of computing the gradient term of the integrated gradient (IG) attribution in Eq. 12, we propose using a score function estimator $s_{X_n}(\mathbf{z}; \theta)$ with parameters θ to directly output the gradient of an outlier measure at node X_n with respect to its input noise vector \mathbf{z} . This approach is more efficient and does not require access to the density function p_Z , which may be unknown or intractable. First, let us define a new outlier attribution measure that relies on this score function estimator, after which we will describe the motivation behind these choices.

Definition 1. Score-based Outlier Measure. Assume the causal structure as in Section II, and $x_n = f(\mathbf{z})$ as in Eq. 6. The score-based outlier measure at leaf X_n , denoted as $S_{X_n}(\mathbf{z})$, is defined as the negative log of the density of X_n :

$$S_{X_n}(\mathbf{z}) = -\log p_{X_n}(x_n) = -\log p_{X_n}(f(\mathbf{z})) \quad (13)$$

In order to compute the gradient of this outlier measure for outlier attribution, we use a score function estimator $s^n(\mathbf{z}; \theta)$ (with a lowercase “ s ”) with parameters θ to predict the gradient of the log density at node X_n , defined as $s^n(\mathbf{z}; \theta) = \nabla_{\mathbf{z}} \log p_{X_n}(f(\mathbf{z}))$. We will describe how to train this model later.

Definition 2. Baseline Outlier Attribution. Let \mathbf{x} be a target outlier with an observed outlier score $S_{X_n}(\mathbf{z})$ at leaf X_n , and let \mathbf{z} be its inverse noise (Eq. 5). Let $\mathbf{z}' \sim p_Z$ be a baseline reference, and let $\mathbf{z}(t)|_{t \in [0,1]}$ a path from $\mathbf{z}(0) = \mathbf{z}'$ to $\mathbf{z}(1) = \mathbf{z}$. We define the baseline outlier contribution of a node j to the target outlier score $S_{X_n}(\mathbf{z})$ based on the path integral as:

$$\approx \frac{1}{2}(z_j - z'_j) \int_{z_j(0)}^{z_j(1)} -s_j^n(\mathbf{z}(t); \theta) dz_j(t) \quad (14)$$

where $s_j^n(\mathbf{z}(t); \theta) = \nabla_{z_j} \log p(\mathbf{z})$ is the j -th component of the score estimator at node X_n .

Above equations are similar to Eq. 14 in the prelim section. We reparameterize the integration variable from dt to dz to

facilitate the gradient path integration with respect to the z variable directly and scale it by $1/2$ to emphasize the triangle approximation of the tail probability area. We added this to the revised version.

The Equation (1) and (5) directly measure the tail probability as outlier measure and use it for explaining outlier. This has several drawbacks such as it is intractable due to unknown density or if using empirical estimate it is inconvenient due to data privacy and storage. We showed that by using Equation (11) to measure the log likelihood in combination with integrated gradient of the diffusion paths we can similarly approximate the tail probability as shown in Figure (1) and thus explaining the outlier.

For implementation, we approximate the integration in Eq. 14 by discretizing the path $\mathbf{z}(t)$ into k time steps as follows:

$$\xi_j(\mathbf{z}, \mathbf{z}') \approx (z_j - z'_j) \sum_{i=1}^k -s_j^n(\mathbf{z}(t_k); \theta)(z_j(t_i) - z_j(t_{i-1})) \quad (15)$$

Next, we define the reference-free version of this definition by marginalizing over the baseline variable.

Definition 3. Score-based Outlier Attribution. The marginal outlier contribution of a node j to the target outlier score $S_{X_n}(\mathbf{z})$ is defined as:

$$\xi_j(\mathbf{z}) = \mathbb{E}_{\mathbf{z}' \sim p_{\mathbf{z}}} \xi_j(\mathbf{z}, \mathbf{z}') \quad (16)$$

$$\approx \frac{1}{m} \sum_{\mathbf{z}^{(i)} \sim p_{\mathbf{z}}|_{i \in \{1, \dots, m\}}} \xi_j(\mathbf{z}, \mathbf{z}^{(i)}) \quad (17)$$

where we used m Monte Carlo samples of the reference noise distribution in Eq. 17 to approximate Eq. 16. This score-based attribution definition satisfies the following axioms for our outlier attribution problem [12, 20, 21]:

- **Axiom 1 (Efficiency):** $\sum_{j \in N} \phi_v(j) = v(N) - v(\{\})$
- **Axiom 2 (Linearity):** $\phi_{\alpha u + \beta v} = \alpha \phi_u + \beta \phi_v$ for any value functions u, v and any $\alpha, \beta \in \mathbb{R}$
- **Axiom 3 (Dummy):** $\phi_v(j) = 0$ whenever $v(I \cup j) = v(I)$ for all $I \subseteq N \setminus j$
- **Axiom 4 (Asymmetry):** $\phi_v(i) = v(\{j : \pi(j) \leq \pi(i)\}) - v(\{j : \pi(j) < \pi(i)\})$ where π is a topological order of the given causal graph.

Theorem 1. Properties of the score-based outlier attribution.

The score-based outlier attribution in Definition 3 satisfies the efficiency, linearity, dummy, and asymmetry axioms for the outlier attribution problem.

Proof. **Axiom 1 (Efficiency).** If we absorb the constant $\frac{1}{2}(z_j - z'_j)$ into the outlier measure or the score function, Eq. 16 becomes:

$$\xi_j(\mathbf{z}, \mathbf{z}') = \int_{z_j(0)}^{z_j(1)} \frac{\partial S_{X_n}(\mathbf{z}(t))}{\partial z_j} dz_j(t)$$

Then,

$$\begin{aligned} \sum_{j \in N} \xi_j(\mathbf{z}, \mathbf{z}') &= \sum_{j \in N} \int_{z_j(0)}^{z_j(1)} \frac{\partial S_{X_n}(\mathbf{z}(t))}{\partial z_j} dz_j(t) \\ &= \int_{\mathbf{z}'}^{\mathbf{z}} \frac{\partial S_{X_n}(\mathbf{z}(t))}{\partial \mathbf{z}} \cdot d\mathbf{z}(t) \\ &= S_{X_n}(\mathbf{z}) - S_{X_n}(\mathbf{z}') \\ &= v(N) - v(\{\}) \end{aligned}$$

where $v(N)$ corresponds to the outlier measure $S_{X_n}(\mathbf{z})$ when *all* components in the outlier noise \mathbf{z} is considered, and $v(\{\})$ corresponds to *none* of the components in the outlier noise \mathbf{z} being considered, i.e., exchanged for the components in the baseline noise \mathbf{z}' . Thus, our attribution method also satisfies the efficiency axiom. The baseline reference-free version of the attribution is achieved by taking the expectation over \mathbf{z}' .

Axiom 2 (Linearity). The Linearity axiom follows from the linearity of the expectation, integration, and derivation operators. Assuming the same setting as in Definition 2, let u and v be two outlier measures as defined in Definition 1, with corresponding score functions $s^n(z(t); \theta_u)$ and $s^n(z(t); \theta_v)$, where θ_u and θ_v are their respectively parameters, and $\alpha, \beta \in \mathbb{R}$. We will show that $\xi(z, z'; \alpha u + \beta v) = \alpha \xi(z, z'; u) + \beta \xi(z, z'; v)$, where the dependence of the attribution ξ on the outlier measure is explicitly shown in its argument. For each node j , we have:

$$\begin{aligned} \xi_j(\mathbf{z}, \mathbf{z}'; \alpha u + \beta v) &= \\ &= \frac{1}{2}(z_j - z'_j) \int_{z_j(0)}^{z_j(1)} \frac{\partial(\alpha u + \beta v)(\mathbf{z}(t))}{\partial z_j} dz_j(t) \\ &= \frac{1}{2}(z_j - z'_j) \int_{z_j(0)}^{z_j(1)} \left(\alpha \frac{\partial u(\mathbf{z}(t))}{\partial z_j} + \beta \frac{\partial v(\mathbf{z}(t))}{\partial z_j} \right) dz_j(t) \\ &= \frac{1}{2}(z_j - z'_j) \int_{z_j(0)}^{z_j(1)} \left(\alpha \frac{\partial u(\mathbf{z}(t))}{\partial z_j} + \beta \frac{\partial v(\mathbf{z}(t))}{\partial z_j} \right) dz_j(t) \\ &= \frac{1}{2} \alpha(z_j - z'_j) \int_{z_j(0)}^{z_j(1)} \frac{\partial u(\mathbf{z}(t))}{\partial z_j} dz_j(t) \\ &\quad + \frac{1}{2} \beta(z_j - z'_j) \int_{z_j(0)}^{z_j(1)} \frac{\partial v(\mathbf{z}(t))}{\partial z_j} dz_j(t) \\ &= \alpha \xi_j(\mathbf{z}, \mathbf{z}'; u) + \beta \xi_j(\mathbf{z}, \mathbf{z}'; v) \end{aligned}$$

This holds of all node $j \in N$. Therefore, the outlier attribution method is linear with respect to the outlier measure. The baseline reference-free version of the attribution is achieved by taking expectation over \mathbf{z}' .

Axiom 3 (Dummy). The Dummy axiom follows from the zero derivative of constant functions. Suppose $v(I \cup j) = v(I)$ for all $I \subseteq N \setminus j$. This means that the outlier measure v is independent of the input dimension j . Therefore, the partial derivative $\partial v(\mathbf{z}(t))/\partial z_j = 0$ for any $\mathbf{z}(t)$. As a result, $\phi(j; v) = 0$.

Axiom 4 (Asymmetry). The discrepancy arises from the different sensitivities of the leaf with respect to these nodes, as shown in the chain rules in Eq. 19, 20, and 21. Thus, similar noise values or changes may be suppressed or magnified when

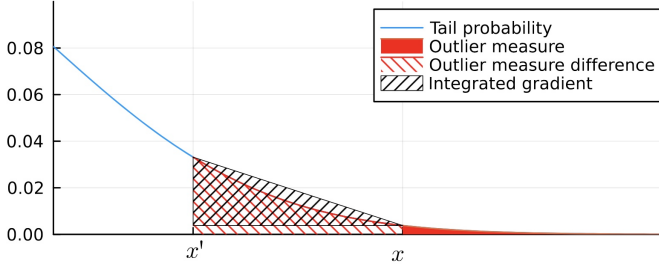


Fig. 1. Outlier measure difference between a target outlier x and a reference point x' as the difference in tail probabilities. For score-based outlier attribution, the expected contribution is the triangle area which is approximately the difference in tail probability $p(X \geq x') - p(X \geq x)$.

they reach the leaf node. A similar point has also been raised in explaining neural network predictions [12]. \square

We now provide a non-rigorous motivation behind these definitions by characterizing the expected change of the tail probability area when moving from an outlier point x to an in-distribution point x' . Let us assume a simple setting where $X = X_n = Z_j$ for all j . Let p_X be a continuously differentiable density function. Then, by using the fundamental theorem of calculus, we can express the expectation of the path integral as the difference in density multiplied by the path distance:

$$\begin{aligned} \mathbb{E}_{p_{X_t}} \frac{1}{2}(x - x') \int_{x'}^x \frac{\partial S_X(x_t)}{\partial x_t} dx_t \\ = \frac{1}{2}(x - x') \int_{x'}^x p_{X_t}(x_t) \frac{-\partial \log p_{X_t}(x_t)}{\partial x_t} dx_t \\ = \frac{1}{2}(x - x') \int_{x'}^x \frac{-\partial p_{X_t}(x_t)}{\partial x} dx_t \\ = \frac{1}{2}(x - x')(p_{X_t}(x') - p_{X_t}(x)) \end{aligned} \quad (18)$$

Eq. 18 represents the area of the triangle with base $x - x'$ and height $p_{X_t}(x') - p_{X_t}(x)$. Fig. 1 illustrates how this triangle area approximates the difference in tail probabilities between the outlier x and the normal x' . Since tail probability indicates the extremeness of x , the increase in tail probability from the outlier x to a normal x' represents the contribution of x to the outlier measure when x is to be exchanged for a normal x' . This explanation aligns with the Shapley values in Eq. 11 where the contribution of a noise z_j , denoted as $\phi_v(j|I)$, is the difference between the outlier measure when z_j is included, $v(I \cup j)$, and when it is excluded, $v(I)$ - that is, when it is exchanged for a normal z'_j .

B. Score Function Estimator

Now, we describe the method to estimate the score function $s^n(\mathbf{z}; \theta)$ with parameters θ to predict the gradient of the log density for a node n w.r.t. the noise vector \mathbf{z} in Eq. 14. Here, we will estimate a set of score functions $\{s^i(\mathbf{z}; \theta)\}_{i=1, \dots, n}$ for every node i in the graph G , given its ancestor noise vector \mathbf{z} . Next, we will analyze and derive an efficient score estimation using conditional score matching.

1) *Conditional Score Matching (CSM):* First, the conditional density function of a node X_i given its parent nodes can be written as follows:

$$p_{X_i}(x_i | x_{\mathbf{Pa}_i}) = p_{Z_i}(z_i | x_{\mathbf{Pa}_i}) = p_{Z_i}(x_i - f_i(x_{\mathbf{Pa}_i}))$$

where the noise $z_i = x_i - f_i(x_{\mathbf{Pa}_i})$ is assumed to have a zero-mean density p_{Z_i} . Therefore, the density p_{X_i} depends on both the observation x_i , the mean function f_i and observation of the parent observations of the parent nodes $x_{\mathbf{Pa}_i}$. Recursively, through f_i and $x_{\mathbf{Pa}_i}$, p_{X_i} depends on all ancestor noise sources, denoted as $\mathbf{z} = \mathbf{z}_{\leq i}$, where $\leq i$ indicates the indices of node i and its ancestor nodes. The score function of x_i w.r.t. z_j , $j \leq i$, can be written as follows:

(i) If $j = i$ then:

$$\begin{aligned} s_i^i(x_i | x_{\mathbf{Pa}_i}) &= \nabla_{z_i} \log p_{X_i}(x_i | x_{\mathbf{Pa}_i}) \\ &= \nabla_{z_i} \log p_{Z_i}(x_i - f_i(x_{\mathbf{Pa}_i})) \\ &= \frac{\partial \log p_{Z_i}(x_i - f_i(x_{\mathbf{Pa}_i}))}{\partial z_i} \\ &= \frac{\partial \log p_{Z_i}(z_i)}{\partial z_i} \end{aligned} \quad (19)$$

(ii) If $j \in \mathbf{Pa}_i$ then:

$$\begin{aligned} s_j^i(x_i | x_{\mathbf{Pa}_i}) &= \nabla_{z_j} \log p_{X_i}(x_i | x_{\mathbf{Pa}_i}) \\ &= \nabla_{z_j} \log p_{Z_i}(x_i - f_i(x_{\mathbf{Pa}_i})) \\ &= \frac{\partial \log p_{Z_i}(x_i - f_i(x_{\mathbf{Pa}_i}))}{\partial z_i} \frac{(-\partial f_i(x_{\mathbf{Pa}_i}))}{\partial z_j} \\ &= \frac{\partial \log p_{Z_i}(z_i)}{\partial z_i} \frac{(-\partial f_i(x_{\mathbf{Pa}_i}))}{\partial x_j} \\ &= s_i^i(x_i | x_{\mathbf{Pa}_i}) \frac{(-\partial f_i(x_{\mathbf{Pa}_i}))}{\partial x_j} \end{aligned} \quad (20)$$

(iii) If $j < i$ is not a direct parent of i , then j has children \mathbf{Ch}_j and the score recursively decomposes with respect to each node $k \in \mathbf{Ch}_j$ as:

$$\begin{aligned} s_j^i(x_i | \mathbf{x}_{<i}) &= \nabla_{z_j} \log p_{X_i}(x_i | \mathbf{x}_{<i}) \\ &= \sum_{k \in \mathbf{Ch}_j} \nabla_{z_k} \log p_{X_i}(x_i | \mathbf{x}_{<i}) \frac{\partial x_k}{\partial z_j} \\ &= \sum_{k \in \mathbf{Ch}_j} s_k^i(x_i | \mathbf{x}_{<i}) \frac{\partial f_k(x_{\mathbf{Pa}_k})}{\partial z_j} \\ &= \sum_{k \in \mathbf{Ch}_j} s_k^i(x_i | \mathbf{x}_{<i}) \frac{\partial f_k(x_{\mathbf{Pa}_k})}{\partial x_j} \end{aligned} \quad (21)$$

As a result, the score function estimator only need to predict the single score $\partial \log p_{Z_i}(z_i) / \partial z_i$ for each z_i . The score for the remaining noises $\mathbf{z}_{<i}$ can then be computed using the chain rules (ii) and (iii) above. Therefore, we will use two set of estimation models, (1) the score models $\{s^i(z_i; \theta_i)\}_{i=1, \dots, n}$ with parameters $\{\theta_i\}_{i=1, \dots, n}$; and (2) the mean models $\{f_i(\mathbf{x}_{\mathbf{Pa}_i}; \phi_i)\}$ with parameters $\{\phi_i\}_{i=1, \dots, n}$. We will describe how to train the score models and the mean models next. Then, we will use an automatic differentiation library to compute the partial derivatives $\partial f_i / \partial x_j$ for each mean model f_i in the experiments.

2) *Sampling Data and Gradient Paths*: To perform outlier attribution using our trained score networks (see Section III-A), we first define the joint score function over all nodes $i = 1, \dots, n$ as

$$\mathbf{s}(\mathbf{z}, t; \theta) = [s^1(z_1, t; \theta_1), \dots, s^n(z_n, t; \theta_n)]^T,$$

where each s^i operates on its local input z_i and produces a gradient estimate. Given an outlier sample \mathbf{z} , we sample m in-distribution trajectories $\{\mathbf{z}^{(k)}(t)\}_{k=1}^m$ by simulating the reverse-time SDE,

$$d\mathbf{z} = -\sigma^2(t)\mathbf{s}(\mathbf{z}, t; \theta) dt + \sigma(t) d\mathbf{w}, \quad (22)$$

using Euler–Maruyama integration [24]. These trajectories interpolate between the outlier and the distributional manifold.

Along each trajectory, we compute the gradient of the log-likelihood via integrated gradients, and apply the chain rules from Eqs. 19–21 to estimate the influence of each latent variable Z_j on the outlier X_n . This yields a Monte Carlo estimate of the attribution score in Eq. 17.

Algorithm 1 provides the detailed procedure for sampling diffusion trajectories and storing the score vectors and diffusion steps. Unlike generative score-based models, we explicitly integrate along the reverse SDE to approximate a path integral over the log-density gradients, enabling principled attribution back to latent noise sources. This latent-space attribution approach distinguishes our method from prior work operating over observed variables.

Algorithm 1 Sampling Trajectories and Storing Gradients and Diffusion Steps

- 1: **input:** trained score network $s_\theta(z, t)$, initial input sample z_0 , time steps t_1, \dots, t_n , time step size Δt , maximum diffusion scale σ_{\max} .
- 2: **init:** initial sample for reverse diffusion $z \leftarrow z_0$, set of scores $\mathcal{S} \leftarrow \emptyset$, set of diffusion steps $\mathcal{D} \leftarrow \emptyset$.
- 3: **for** $i = 1$ to n **do**
- 4: $\sigma^2 \leftarrow (\sigma_{\max}^{2t_i} - 1)/(2 \log \sigma_{\max})$ {Diffusion coefficient}
- 5: $\nabla z \leftarrow s_\theta(z, t_i)$ {Evaluate score at z }
- 6: $\mu_z \leftarrow z + \sigma^2 \cdot \nabla z \cdot \Delta t$ {Euler–Maruyama mean update}
- 7: $z_{\text{new}} \leftarrow \mu_z + \sigma \cdot \sqrt{\Delta t} \cdot \epsilon$, where $\epsilon \sim \mathcal{N}(0, I)$ {Add Gaussian noise}
- 8: $\mathcal{S} \leftarrow \mathcal{S} \cup \{\nabla z\}$ {Store score vector}
- 9: $dz_i \leftarrow z_{\text{new}} - z$ {Compute diffusion step}
- 10: $\mathcal{D} \leftarrow \mathcal{D} \cup \{dz_i\}$ {Store diffusion step}
- 11: $z \leftarrow z_{\text{new}}$ {Set new z }
- 12: **end for**
- 13: **return** score trajectories $\mathcal{S} = \{\nabla s(z, t_i)\}_i$ of shape (d, n) and diffusion steps $\mathcal{D} = \{dz_i\}_i$ of shape (d, n) .

3) *Fitting Mean Models*: While the score-based framework in Section 3.2.3 enables the attribution of an outlier observation z to the underlying latent perturbations via gradient paths, it does not by itself quantify how these perturbations propagate through the structural causal model. To estimate

such propagation effects, particularly how noise sources Z_j influence downstream variables X_i , we must recover the functional relationships f_i that define the structural assignments $X_i = f_i(\mathbf{Pa}_i) + Z_i$. These impact functions f_i provide a functional semantics to the directed edges in the causal graph. Thus, we fit the regression models for each node i as described below.

For each node i , we use a regression neural networks with parameters ϕ_i for modeling the mean $\mathbb{E}X_i = \mathbb{E}(f_i(X_{\mathbf{Pa}_i}; \phi_i) + Z_i) = f_i(X_{\mathbf{Pa}_i}; \phi_i)$, where we assume zero mean noise Z_i . We train the network using regularized regression:

$$\phi_i^* = \underset{\phi_i}{\operatorname{argmin}} \mathbb{E}_{\mathbf{x}} \|\mathbf{x}_i - f_i(\mathbf{x}_{\mathbf{Pa}_i})\|^2 + \eta \|\phi_i\|^2$$

where η is regularization parameter.

In the case of additive noise model, the additive noise model fit reduces to MSE error as mentioned above. For the location scale model,

$$p(y | x) = \mathcal{N}(y | \mu_\phi(x), \sigma_\phi(x)^2)$$

we use the following negative log-likelihood objective:

$$\text{NLL}(\phi | x, y) = \frac{(y - \mu_\phi(x))^2}{2\sigma_\phi(x)^2} + \frac{1}{2} \log(\sigma_\phi(x)^2)$$

f_j can be modeled using neural networks trained with mean squared error (MSE) loss $\mathbb{E}[(X_j - f_j(\mathbf{Pa}_j))^2]$. The optimal predictor under this loss is the conditional expectation $f_j(\mathbf{Pa}_j) = \mathbb{E}[X_j | \mathbf{Pa}_j]$, [25, Sec. 1.5.5]. This result holds regardless of the noise distribution. The variance $\text{Var}(X_j | \mathbf{Pa}_j)$, represents the irreducible uncertainty in the target, captured by the noise term Z_j .

C. Discussions

Extending the chain rule decomposition from additive noise models (ANMs), our key contribution is integrating this principle into a diffusion-based attribution framework operating in the latent noise space. By tracing the influence of noise perturbations through diffusion trajectories governed by the reverse SDE in Eq. 22, we enable gradient-based attribution. Unlike prior approaches that compute attribution scores with respect to observed variables, we formulate attribution in terms of latent noise variables using score-based diffusion modeling and Monte Carlo sampling of gradient paths, as detailed in Section III.

Our score-based attribution method inherits desirable properties from the Shapley value framework in cooperative game theory. Specifically, the attribution scores computed via integrated gradients over the negative log-likelihood (NLL) satisfy three of the four classic Shapley axioms—dummy, efficiency, and linearity. The fourth axiom, symmetry, does not generally hold in our setting; instead, we replace it with a context-specific asymmetry property induced by the underlying causal structure, wherein different variables may play inherently asymmetric roles in generating outliers. This theoretical grounding supports the faithfulness of our explanations: outlier nodes receive high attribution scores due to their

disproportionate contributions to log-likelihood deviations. Furthermore, we interpret these scores as being approximately proportional to differences in tail probabilities, which we estimate using a triangle rule over the diffusion gradient path (see Fig. 1).

Following [8], we adopt the mechanism perturbation view of outliers, interpreting them as structural deviations in functional assignments or shifts in the noise-generating process. In the FCM framework, the exogenous noise variable determines the selection of deterministic mechanisms. Therefore, an outlier does not merely correspond to an unusual noise realization but reflects a structural shift in the response function. This view allows us to model outliers as arising from changes in mechanism, not just from stochastic noise. Rather than relying on density-based tail estimates (e.g., Eqs. (1) and (5)), which are often intractable or restricted due to privacy or storage constraints, we use Eq. (11) in conjunction with integrated gradients to approximate the tail probability and explain the outlier behavior effectively.

Interpreting outliers as violations of causal invariance rather than extremal additive noise realizations is a more principled and informative perspective. Our approach is indeed aligned with this interpretation, as in [8] and in [9]. We further extend this idea by incorporating location-scale models, allowing the mean and variance of the noise to depend on the parents, thus supporting heteroscedastic and context-sensitive mechanism changes.

Our framework builds upon standard assumptions in causal inference [8, 15], notably that the data-generating process follows a Functional Causal Model (FCM) structured as a directed acyclic graph (DAG) with causal sufficiency. We assume that the noise variables $\{Z_j\}$ are jointly independent and that the causal mechanisms are locally identifiable, meaning the score functions of the noise distributions and their perturbations are estimable from data, enabling gradient-based inference.

IV. EXPERIMENTS

In this section, we evaluate our method, SIREN, in outlier attribution tasks on random graph datasets and in a micro cloud services scenario. We compare **SIREN** to the following baselines:

- 1) **Naive**: This method simply uses the z -score of the marginal distribution of the observational data of each node X_i as its contribution value to the target outlier measure. The ranking of root causes is based on these z -scores, a higher ranking corresponds to a higher z -score.
- 2) **Traversal**: [6, 7] assumes a root cause is a node whose parent observations are normal, but there is a descendant path of anomalous nodes linking it to the target outlier node.
- 3) **CIRCA**: [18] models the functional causal mechanisms (FCMs) using linear regression with Gaussian noise. The authors compute the residual, Eq. 5, of an outlier observation and use it for ranking root causes.

- 4) **CausalRCA**: [8] fits the FCMs using linear regression. The authors use the Shapley value attribution method to compute the attribution score of each node. They rewrite the target outlier node as a function of all ancestor noises, including itself, Eq. 6. The marginal contribution of each noise source to the target outlier leaf, given all randomized noise contexts is used for ranking root causes.
- 5) **BIGEN**: [9] fits a Bayesian linear regression to the FCMs and use integrated gradients of the noise sources as the leaf outlier contributions for ranking root causes.

A. Random Graph Datasets

Hyper-parameters for SIREN in Table. I

Network	Number of layers	Hidden size	Activation
mean model f_j	2	100	tanh
location model μ_j	2	100	tanh
scale model σ_j	2	100	0.5 + tanh
score model s_j	3	100	swish

TABLE I
NETWORK ARCHITECTURE DETAILS FOR SIREN.

BIGEN, CausalRCA, CIRCA, and Traversal use a similar model as the mean model f_j . The BIGEN model uses Gaussian Dropout to multiply each activation by noise sampled from a Gaussian distribution with mean 1.0 and standard deviation 0.1. All training is done using the Adam optimizer with default parameters in 100 epochs.

In this experiment, we use random graph datasets to compare the performance of all methods. We randomly generate 100 causal graphs with varying number of nodes in the range from 50 to 100. For each graph, we select the subgraph with a depth of at least 10 and having only one leaf for study. For the FCMs, we use 3-layer MLPs with 50 hidden units and a ReLU activation function in the hidden layer. We then draw normal data from these FCMs, following the causal structure. To synthesize the outliers, we randomly select between 1 to 3 nodes as root causes. We inject outlier noise into the nodes to create the ground truths by changing the scale of these noise sources three times. The noise distribution for each FCM is randomly selected as a mixture of Gaussians with 2 components, with means sampled from $\mathcal{N}(0, 1)$, both having the same variance of 1, and the prior weights are $[\alpha, 1 - \alpha]$, where $\alpha \in [0.1, 0.9]$.

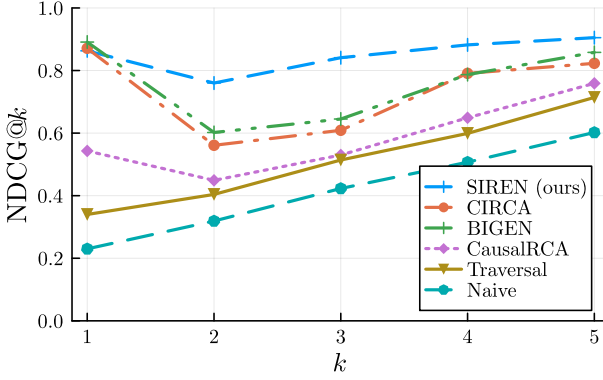
Table. II compares the average NGCG@ k ranking on random graph datasets. SIREN outperforms all the baselines in root cause detection ranking on average across top- k measures. CIRCA and BIGEN perform comparably and are better than CausalRCA, Traversal, and Naive method.

Fig. 2 shows the detailed top- k rankings of the methods. At the top-1 ranking, all three methods - SIREN, CIRCA, and BIGEN - correctly detect the first root cause, performing closely at about 83%. However, for the top-2 and top-3 rankings, only SIREN maintains accurate rankings, while CIRCA and BIGEN drop to about 60% NGCG score. This suggests that

	Average NGCG@ k ranking
SIREN (ours)	85.0 \pm 11.5
CIRCA	73.1 \pm 18.1
BIGEN	75.7 \pm 17.5
CausalRCA	58.6 \pm 18.3
Traversal	51.4 \pm 21.8
Naive	41.6 \pm 19.6

TABLE II

AVERAGE NGCG@ k RANKING IN THE ROOT CAUSE ATTRIBUTION TASK ON RANDOM GRAPH DATASETS.

Fig. 2. NDCG@ k ranking across different k values.

the data distribution is complex and requires better distribution matching to detect more than one root cause in ancestor nodes. SIREN's score matching ability gives it an advantage in this case. At higher top- k rankings, all methods seem to converge, but SIREN still performs the best among the six methods.

B. Root Causes of Cloud Service Latencies

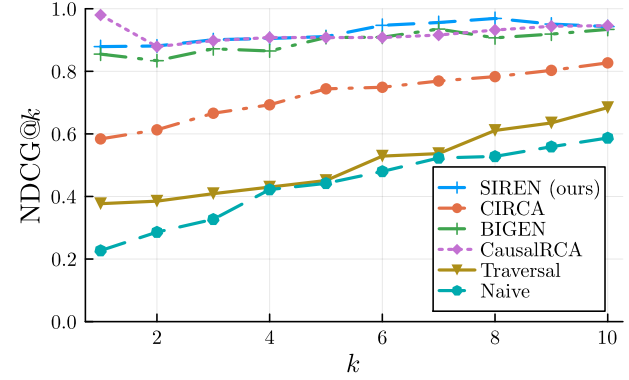
In this experiment, we compare our methods with the baselines in a simpler, realistic scenario within a small microservice environment. Specifically, we investigate and identify the root causes of observed latencies in cloud services for an online shop [26–28]. We consider normal random delay noises at each service X_j to be sampled from a half-normal distribution with a mean between 100–500 ms and a scale between 100–200 ms. We randomly select between 1–3 nodes and change their means and noise scales three times. Our objective is to identify the root causes of unwanted latency experienced by customers when processing online orders. This service interacts with multiple other web services, which are represented by a causal dependency graph that includes ten additional services [28]. We assume that we are observing latencies in the order confirmation at the website's leaf node, and that all services operate in synchronization. We use similar models as in the previous section for this experiment, assuming the causal graph is given, and fit the noisy FCM models to the training data collected during normal operations. Due to the linearity of the problem, we use linear regression instead of neural network for fitting the mean functions in SIREN.

Table III compares the root cause rankings of all methods. It shows that SIREN, BIGEN, and CausalRCA can correctly rank root causes of delays on average for these online shop

	Average NGCG@ k ranking
SIREN (ours)	92.1 \pm 3.3
CIRCA	72.3 \pm 8.1
BIGEN	89.4 \pm 3.7
CausalRCA	92.2 \pm 2.9
Traversal	50.4 \pm 3.6
Naive	43.8 \pm 12.2

TABLE III

AVERAGE NDCG@ k RANKING IN AN ONLINE SHOP CLOUD SERVICE.

Fig. 3. NDCG@ k with varying the number of k .

cloud services. CIRCA performs reasonably, achieving 72.3% NDCG@ k on average, which may be due to the difficulty posed by asymmetric noise sources, making it fail in this context because it simply uses the z -score with the fitted mean function. This creates additional challenges for the Traversal and Naive methods.

Fig. 3 shows that CausalRCA can perfectly rank the first root cause, while it is comparable to SIREN and BIGEN for larger k . All methods exhibit better NDCG@ k scores with larger k values, as the chances of relevant root causes appearing increase.

C. Root Causes of Supply Chain Latencies

In this experiment, we simulated a supply chain latency dataset with the interactions between vendors and retailers. The real-world delays and decision-making overheads introduce stochastic variability. This experiment captures realistic structural dependencies, time-lagged effects, and non-additive noise patterns that arise in business operations and logistics, closely mirroring real causal phenomena. The results showed that our model effectively identifies latent root causes of outliers observed at the final "Received" node, and outperforms baseline methods on NDCG@ k metrics (Table 2), showing robustness and accuracy in attribution under realistic noise and delay distributions.

We based on the root cause analysis in a real world supply chain scenario using the simulator in [Nguyen et al., 2024]. This experiment addresses the challenge of identifying root causes of outlier events (e.g. delays) in a supply chain system. The setting simulates a realistic retail-vendor chain with stochastic delays, modeled using location scale data generating

process. The supply chain works as follow. A retailer places orders based on forecasted demand and inventory constraints. A vendor then confirms orders and ships goods with random delays. The delays simulate business overheads like managerial decisions or variable operations. Outliers are injected by perturbing the noise, e.g. Uniform(3, 5). The objective is to identify the root causes of outliers at the final node (Received) by ranking influential upstream variables. Table IV shows the average NDCG@k ranking results from different runs:

TABLE IV
NDCG@K RANKING ACROSS FIVE K VALUES BY DIFFERENT METHODS

Method	k=1	k=2	k=3	k=4
SIREN	92.7 ± 2.1	81.6 ± 6.7	80.4 ± 7.0	82.0 ± 5.2
CIRCA	71.0 ± 41.6	72.0 ± 27.3	73.7 ± 18.5	80.5 ± 15.7
BIGEN	56.8 ± 43.2	56.9 ± 36.3	63.6 ± 29.2	72.5 ± 21.5
CausalRCA	77.0 ± 22.0	68.1 ± 16.1	65.5 ± 12.5	71.6 ± 12.6
Traversal	62.8 ± 31.5	70.3 ± 25.4	73.7 ± 20.3	77.7 ± 14.3
Naive	53.5 ± 29.5	61.1 ± 18.9	64.4 ± 13.9	69.8 ± 7.7

V. RELATED WORK

A closely related method to ours is BIGEN [9], in which the authors also use integrated gradients for root cause attribution. However, their method only works for linear Gaussian FCMs, which limits root cause analyses to linear and Gaussian noise assumptions. They also require access to the training data for attribution. Another closely related method is the pioneering CausalRCA [8], where the authors base their approach on the causal structure of the data and use Shapley values for outlier attribution. However, this method requires linear FCMs, and training data for root cause attribution, and its computation is expensive. CIRCA [18] models the data using linear FCMs and uses the distance to the predicted mean for ranking root causes. [10] utilize the topological order of a causal structure and consider only a single root cause. The authors proposed to traverse the nodes in reverse topological order and use changes in log probabilities to identify the root cause. Earlier methods employing the traversal approach include [6, 7, 29]. However, these methods use a heuristic algorithm to identify a root cause by checking its parents for non-anomalous activity and finding a path of anomalous nodes linking to the target outlier.

VI. CONCLUSION

We proposed SIREN, a score-based integrated gradient framework for root cause attribution in complex, noisy systems. SIREN attributes an outlier measure at a leaf node to its ancestor nodes via integrated gradients, identifying likely root causes. Our framework is built upon a conditional score matching model that enables efficient computation of integrated gradient-based outlier scores, facilitated by a decomposed score function. Unlike prior methods, SIREN supports nonlinear, heteroscedastic causal models by modeling location-scale noise and interpreting outliers as violations of causal invariance rather than extreme noise realizations. Extensive theoretical analysis and empirical evaluations confirm the effectiveness, scalability, and interpretability of our approach.

REFERENCES

- [1] Dragan Djurdjanovic, Jay Lee, and Jun Ni. Watchdog agent an infotronics based prognostics approach for product performance degradation assessment and prediction. *Advanced Engineering Informatics*, 17(3-4):109–125, 2003.
- [2] Jingchao Ni, Wei Cheng, Kai Zhang, Dongjin Song, Tan Yan, Haifeng Chen, and Xiang Zhang. Ranking causal anomalies by modeling local propagations on networked systems. In *2017 IEEE ICDM*, pages 1003–1008. IEEE, 2017.
- [3] Jamie Pool, Ebrahim Beyrami, Vishak Gopal, Ashkan Aazami, Jayant Gupchup, Jeff Rowland, Binlong Li, Pritesh Kanani, Ross Cutler, and Johannes Gehrke. Luminos: A library for diagnosing metric regressions in web-scale applications. In *26th ACM SIGKDD*, pages 2562–2570, 2020.
- [4] Jaehyuk Yi and Jinkyoo Park. Semi-supervised bearing fault diagnosis with adversarially-trained phase-consistent network. In *27th ACM SIGKDD*, pages 3875–3885, 2021.
- [5] Amin Dhaou, Antoine Bertoncello, Sébastien Gourvénec, Josselin Garnier, and Erwan Le Pennec. Causal and interpretable rules for time series analysis. In *27th ACM SIGKDD*, pages 2764–2772, 2021.
- [6] Jinjin Lin, Pengfei Chen, and Zibin Zheng. Microscope: Pinpoint Performance Issues with Causal Graphs in Micro-service Environments. In Claus Pahl, Maja Vukovic, Jianwei Yin, and Qi Yu, editors, *Service-Oriented Computing*, volume 11236, pages 3–20. Springer International Publishing, Cham, 2018. Series Title: Lecture Notes in Computer Science.
- [7] Dewei Liu, Chuan He, Xin Peng, Fan Lin, Chenxi Zhang, Shengfang Gong, Ziang Li, Jiayu Ou, and Zheshun Wu. Microhecl: High-efficient root cause localization in large-scale microservice systems. In *2021 IEEE/ACM 43rd International Conference on Software Engineering: Software Engineering in Practice (ICSE-SEIP)*, pages 338–347. IEEE, 2021.
- [8] Kailash Budhathoki, Lenon Minorics, Patrick Blöbaum, and Dominik Janzing. Causal structure-based root cause analysis of outliers. In *Proceedings of the 39th International Conference on Machine Learning*, volume 162 of *Proceedings of Machine Learning Research*, pages 2357–2369. PMLR, 2022.
- [9] Phuoc Nguyen, Tryuyen Tran, Sunil Gupta, Thin Nguyen, and Svetha Venkatesh. Root Cause Explanation of Outliers under Noisy Mechanisms. In *Proceedings of the AAAI Conference on Artificial Intelligence*, volume 38, pages 20508–20515, 2024.
- [10] Nastaran Okati, Sergio Hernan Garrido Mejia, William Roy Orchard, Patrick Blöbaum, and Dominik Janzing. Root Cause Analysis of Outliers with Missing Structural Knowledge, June 2024.
- [11] Ahsan Mahmood, Junier Oliva, and Martin Styner. Mul-

tiscale score matching for out-of-distribution detection. *arXiv preprint arXiv:2010.13132*, 2020.

[12] Christopher Frye, Colin Rowat, and Ilya Feige. Asymmetric shapley values: incorporating causal knowledge into model-agnostic explainability. *Advances in neural information processing systems*, 33:1229–1239, 2020.

[13] Tom Heskes, Evi Sijben, Ioan Gabriel Bucur, and Tom Claassen. Causal shapley values: Exploiting causal knowledge to explain individual predictions of complex models. *Advances in neural information processing systems*, 33:4778–4789, 2020.

[14] Judea Pearl. *Causality: Models, Reasoning, and Inference*. Cambridge University Press, Cambridge, UK, 2nd edition, 2009.

[15] Jonas Peters, Dominik Janzing, and Bernhard Schölkopf. *Elements of causal inference: foundations and learning algorithms*. The MIT Press, 2017.

[16] Patrik O. Hoyer, Dominik Janzing, Joris M. Mooij, Jonas Peters, and Bernhard Schölkopf. Nonlinear causal discovery with additive noise models. *Neural Information Processing Systems (NeurIPS)*, 21:689–696, 2009.

[17] Peter Bühlmann, Jonas Peters, and Jan Ernest. Cam: Causal additive models, high-dimensional order search and penalized regression. *Annals of Statistics*, 42(6):2526–2556, 2014.

[18] Mingjie Li, Zeyan Li, Kanglin Yin, Xiaohui Nie, Wenchi Zhang, Kaixin Sui, and Dan Pei. Causal Inference-Based Root Cause Analysis for Online Service Systems with Intervention Recognition. In *Proceedings of the 28th ACM SIGKDD Conference on Knowledge Discovery and Data Mining*, pages 3230–3240, Washington DC USA, August 2022. ACM.

[19] Biwei Huang, Kun Zhang, and Bernhard Schölkopf. Generalized score functions for causal discovery. In *Proceedings of the 21st ACM SIGKDD International Conference on Knowledge Discovery and Data Mining*, pages 1551–1560. ACM, 2015.

[20] Lloyd S Shapley. A value for n-person games. In Harold W. Kuhn and Albert W. Tucker, editors, *Contributions to the Theory of Games*, volume 2 of *Annals of Mathematics Studies*, pages 307–317. Princeton University Press, Princeton, NJ, 1953.

[21] Mukund Sundararajan and Amir Najmi. The many shapley values for model explanation. In Hal Daumé III and Aarti Singh, editors, *Proceedings of the 37th International Conference on Machine Learning*, volume 119 of *Proceedings of Machine Learning Research*, pages 9269–9278. PMLR, 13–18 Jul 2020.

[22] John Von Neumann and Oskar Morgenstern. Theory of games and economic behavior: 60th anniversary commemorative edition. In *Theory of games and economic behavior*. Princeton university press, 2007.

[23] Scott M. Lundberg and Su-In Lee. A unified approach to interpreting model predictions. In Isabelle Guyon, Ulrike von Luxburg, Samy Bengio, Hanna Wallach, Rob Fergus, S. V. N. Vishwanathan, and Roman Garnett, editors, *Advances in Neural Information Processing Systems*, volume 30, pages 4765–4774. Curran Associates, Inc., 2017.

[24] Yang Song, Jascha Sohl-Dickstein, Diederik P. Kingma, Abhishek Kumar, Stefano Ermon, and Ben Poole. Score-Based Generative Modeling through Stochastic Differential Equations, February 2021.

[25] Christopher M. Bishop. *Pattern Recognition and Machine Learning*. Springer, New York, 2006.

[26] Feiyan Guo, Bing Tang, and Mingdong Tang. Joint optimization of delay and cost for microservice composition in mobile edge computing. *World Wide Web*, 25(5):2019–2047, 2022.

[27] Azam Ikram, Sarthak Chakraborty, Subrata Mitra, Shiv Saini, Saurabh Bagchi, and Murat Kocaoglu. Root cause analysis of failures in microservices through causal discovery. *NeurIPS*, 35:31158–31170, 2022.

[28] Patrick Blöbaum, Peter Götz, Kailash Budhathoki, Atlanti A. Mastakouri, and Dominik Janzing. Dowhy-gcm: An extension of dowhy for causal inference in graphical causal models. *arXiv preprint arXiv:2206.06821*, 2022.

[29] Pengfei Chen, Yong Qi, Pengfei Zheng, and Di Hou. Causeinfer: Automatic and distributed performance diagnosis with hierarchical causality graph in large distributed systems. In *IEEE INFOCOM 2014-IEEE Conference on Computer Communications*, pages 1887–1895. IEEE, 2014.